Demand Response Modeling in Microgrid Operation: a Review and Application for Incentive-Based and Time-Based Programs

Mahmood Hosseini Imani[*], M. Jabbari Ghadi[#], Sahand Ghavidel[#], Li Li[#]

[*]Department of Electrical Engineering, Faculty of Engineering, University of Guilan, Rasht, Iran.

[#] Faculty of Engineering and Information Technology, University of Technology Sydney, Australia

[*]Email: Hosseini@msc.guilan.ac.ir

[#]Email: {Mojtaba.jabbarighadi, Sahand.ghavideljirsaraie}@student.uts.edu.au, {li.li}@uts.edu.au

Abstract

During recent years, with the advent of restructuring in power systems as well as the increase of electricity demand and global fuel energy prices, challenges related to implementing demand response programs (DRPs) have gained remarkable attention of independent system operators (ISOs) and customers, aiming at the improvement of attributes of the load curve and reduction of energy consumption as well as benefiting customers.

In this paper, different types of DRPs are modeled based on price elasticity of the demand and the concept of customer benefit. Besides, the impact of implementing DRPs on the operation of grid-connected microgrid (MG) is analyzed. Moreover, several scenarios are presented in order to model uncertainties interfering MG operations including failure of generation units and random outages of transmission lines and upstream line, error in load demand forecasting, uncertainty in production of renewable energies (wind and solar) based distributed generation units, and the possibility that customers do not respond to scheduled interruptions.

Simulations are conducted for two principal categories of DRP including incentive-based programs and time-based programs on an 11-bus MG over a 24-hour period and also a 14-bus MG over a period of 336 hours (two weeks). Simulation results indicate the effects of DRPs on total operation costs, customer's benefit, and load curve as well as determining optimal use of energy resources in the MG operation. In this regard, prioritizing of DRPs on the MG operation is required.

Index Terms

Microgrid (MG), Demand response programs (DRPs), System operation, Distributed generation.

[#]Corresponding Author: M. Jabbari Ghadi; Postal address: Faculty of Engineering and Information Technology, University of Technology, Sydney, PO Box 123, Broadway, NSW 2007, Australia;

Phone: +61- 466996685, E-mail: Mojtaba.JabbariGhadi@uts.edu.au

Nomenclature

b	Index of battery
i,j	Index of bus
s	Index of scenario
t	Index of time
z	Index of time period
a_{mt}, b_{mt}	Coefficients of cost of Micro-turbines (MTs)
A_z	Incentive price that is paid to the costumer in time period z
$A_{i,t}$	Incentive price that is paid to the costumer in time t at bus i
B_z^0	Customer's income in period z
$C_{i,t,s}^{DR}$	Cost of implementing the DRP (sum of rewards received by customer)
d_z , $d_{z'}$	Load demand in period z and z'
$DR_{i,t,s}^{-}$	Load reduction at bus i at time t and scenario s
$DR_{i,t,s}^{+}$	The shifted load to an off-peak hour at bus i at time t and scenario s
$D_{i,z}, D_{i,z'}$	Total load of bus i of the z^{th} and z'^{th} period
E_{zz}	Self-elasticity of period z
$E_{zz'}$	Cross elasticity of period z to period z'
$E_{z'z'}$	Self-elasticity of period z'
$E_{b,t,s}^{B}$	Remaining capacity (battery energy) at time t and scenario s
$E_b^{B,\min}, E_b^{B,\max}$	Minimum and maximum permissible battery capacity
$G_{i,j}$, $B_{i,j}$	The line conductance and susceptance (from bus i to j)
IDR	Set of customers that participated in the DRP
$IC_{i,t,s}$	Customer's response to interruptible/curtailable (I/C) program at bus i at time t and scenario s (0/1)
$LS_{i,t,s}$	Unsupplied load at time t and scenario s and customer i and scenario s
MT_i	MTs connected to bus i

Nmt	Number of MTs
Ni	Number of buses
NS	Number of samples
NT	Time period of DRP
NZ	Number of periods (Zones)
PV	Solar cell units
$P_{b,t,s}^{B}$	Power generation of battery *b* at time *t* and scenario *s*
$P_{i,t,s}^{D}$	The amount of load at bus *i* at time *t* and scenario *s*
$P_{pv,t,s}^{PV}$	Power generation of solar units at time *t* and scenario *s*
$P_{w,t,s}^{W}$	Power generation of wind unit *w* at time *t* and scenario *s*
$P_{i,t,s}^{D}$	Consumed load of bus *i* at time *t* and scenario *s*
$P_{mt}^{MT,\min}, P_{mt}^{MT,\max}$	The maximum and minimum power generation of *MTs*
$P_{w,t,s}^{W,forecast}$	The predicted power generation of wind units, at time *t* and scenario *s*
$P_{pv,t,s}^{PV,forecast}$	The predicted power generation of solar units, at time *t* and scenario *s*
$P^{Grid,\max}$	The maximum exchanged power with up-grid
$P_{mt,t,s}^{MT}$	The MT production power at time *t* and scenario *s*
$P_{i,t,s}^{buy}, P_{i,t,s}^{sell}$	The amount of energy bought from/sold to the up-grid at time *t* and scenario *s*
$PC_{i,t,s}^{IC}$	Customer's penalty at bus *i* at time *t* and scenario *s*
$PP_{i,t}$	The amount of penalty per kW at bus *i* at time *t*
$P_{b,t,s}^{ch}, P_{b,t,s}^{dc}$	Charging and discharging power at time *t* and scenario *s*
$PL_{i,j,t,s}$,	The transferred active power of each transmission lines (from bus *i* to *j*)
$P_{b}^{ch,\min}, P_{b}^{ch,\max}$	Minimum and maximum charge rate of the batteries
$P_{b}^{dc,\min}, P_{b}^{dc,\max}$	Minimum and maximum discharge rate of the batteries
q_0	Initial demand value (kWh)
q	Customer demand (kWh)
q_z , $q_{z'}$	Customer demand of period *z* and period z' (kWh)
$\phi_{pv,t,s}^{PV}$	Solar radiation (kW/m^2)
$QL_{i,j,t,s}$	The transferred reactive power of each transmission lines (from bus *i* to *j*)
S_{pv}^{PV}	The area of each PV unit (m^2)
$SL_{i,j}^{\max}$	Maximum AC Power on a line from bus *i* to *j*
$T_z, T_{z'}$	Sets of times related to period z and period z'; $T_z \cap T_{z'} = \varnothing$ if $z \neq z'$.
$u_{mt,t,s}$	The binary variable that shows the on/off state of MT at time *t* and scenario *s*

$u_{t,s}^{Grid}$	Binary variables indicating the buy/sell state at time *t* and scenario *s*
$u_{b,t,s}^{ch}$, $u_{b,t,s}^{dc}$	Binary variables indicating the battery in charging and discharging mode
$VOLL_{i,t}$	Penalty for unsupplied load
$V_{i,t,s}$	Voltage on bus i at time *t* and scenario *s*
Z_t	Z_t ={z: zth period is related to hour t}; Z_t is a single-element set
λ	Failure rate
μ	Repair rate
$d_{i,t,s}$	Phase angle on bus i at time *t* and scenario *s*
S_z	Costumer's profit in period *z*
Δd_z	Amount of customer's load that changed by customer when he/she receives the incentive
Δd_z^+	Change in the load (load shift) to other periods due to load reduction in period *z*
η_{pv}^{PV}	Solar cell efficiency
h_b^{ch} , h_b^{dc}	The efficiency of charge and discharge of battery storage system
π_s	Probability of scenario *s*
ρ_{0z} , $\rho_{0z'}$	Initial electricity energy price of period *z* and period z' (cent/kWh)
ρ	Electricity energy price (cent/kWh)
ρ_z , $\rho_{z'}$	Electricity energy price of period *z* and period z' (cent/kWh)
ρ_t	Hourly energy price of the up-grid

1 INTRODUCTION

Recntly, environmental concerns, the energy crisis and advances in renewable technologies have caused the increasing use of distributed generation (DG) units in power systems. Despite provision of the significant advantages for power systems, these units may cause some challenges related to the complexity of power system, allocation of protection devices and planning challenges due to the change of traditional structure of distribution systems toward new active ones [1].

One of the proposed views to overcome these challenges and effectively increase the participation of these resources into power systems is the concept of microgrids (MGs). MG increases the observability and control of the network to provide an optimal condition for effective aggregation of these resources into the grid. In fact, MGs are small-scale power systems including micro-turbines (MTs), distributed energy resources (DER), power storages and controllable loads. MGs are entirely under the supervision of an adaptive control and a management system with the capability of operation in grid-connected and islanded conditions [1].

In recent times, research related to the operation of MGs have gained more attention [2-5]. In [2], the scheduling of an MG to maximize the revenue of DG units is explored utilizing some economy factors for selling and purchasing energy for each of generation units and loads. A methodology for cooperating and modeling the market mechanism for MGs is proposed in [3] where the general model of the smart grid from both the functional and architectural viewpoints is described. In [4], the control of an MG based on a decentralized strategy employing a multi-agent system is explained. A symmetrical assignment approach for the optimal exchange of energy among the generating units of MG, the local loads and the upstream grid is presented in this paper. In [5], the daily scheduling of an MG is implemented. First, the total demand of MG should be supplied by local generating units with the minimum power purchase from the upstream. Second, transactions with the upstream are allowed.

One of the concepts which has been developed with the advances in MG operations is demand response (DR). According to the United States Department of Energy (DOE), DR is the modification of consumer's demand for energy through various methods such as financial incentives and behavioral change through education [6]. In fact, the implementation of DR programs (DRPs) in MGs leads to enhancing the MG reliability as well as managing the intermittent impacts of renewable energy sources (RES) [7]. These obligations can be implemented through the reduction of demand during the critical time (*i.e.* some hours over an operation scheduling in which the price of energy in the market has its maximum values or the reserve margin is limited due to the failure of generating units, outage of transmission lines and the inaccessibility to the upstream grid).

To this end, DR resources have been utilized to maintain system reliability during peak load periods due to concerns of significant load growth in California and the western United States region [8]. Several other studies have been conducted for applying DR to the case of insufficient supply in power grids [9,10]. Along with the development of the market operations in electric power systems, the concept of DR started to develop and some new economic programs of DR have been suggested. In [11], the impacts of emergency DRP (EDRP) for reliability improvement for cases of generation units' failures are studied. In [12] the impact of customers' participation level and various incentive values on implementing DRPs in MG operations is investigated. Also, it is seen that illogical decrease or increase of the incentives causes the increase of overall operation cost. Based on the study in [13], a DRP based on time of use (TOU) is proposed to overcome challenges of the optimal pricing during various time periods. This optimal pricing during different periods (*i.e.* valley, off-peak, and peak periods) is obtained through determination of the minimum cost by applying the dynamic economic dispatch. An EDRP and TOU based DR approach is employed in [14] to maximize benefits of customers. However, in this research, the minimization of

the total operating cost as an objective function is not considered. A critical peak pricing (CPP) approach of DR is proposed in [15]. In fact, the CPP is only applied during contingencies or during peak time where the rate structure is different (*e.g.* situations with very high amounts of electricity usage when the information related to the energy price will be received early before the happening of an event by the consumers). In real time pricing (RTP) programs [16], there is an option for consumers to set their hourly load usage according to real-time electricity prices to maximize their profit. This paper uses a decomposition technique based on Lagrangian relaxation to form the model of DR. Economic models for three time-based programs including TOU, RTP, and CPP are extended in [17]. However, incentive-based programs are not studied in this research, and also customer's penalty due to the refusal of load reduction is not mentioned. I/C service as an intensive based program is utilized for customers who accept to reduce their load to predefined levels when it is necessary [15], while there might be a risk of penalty for those participants who decline load reduction. In [18], the customer benefit function and price elasticity of demand are used for the economic model of I/C program. Direct load control (DLC) program is presented in [19,20] which uses a remote access to the switch of controllable loads (*e.g.* water heaters and air conditioners). A model for maximizing consumer comfort is suggested in them which controls individual storage device in response to price signals. The authors in [21] apply a methodology to obtain a priority list for DRPs in a power market to reach the maximum customers' profit. However, it does not consider the operational constraints of both MG and DR models.

Afterward, a large number of studies have been conducted to involve DR aggregators into MGs with different models of DR and objectives. In [22], the profit maximization bidding strategy is considered for MG and DR based on a risk-constrained stochastic programming framework. Authors in [23] model energy storage systems in the simultaneous scheduling of MG and DR to deal with uncertainties associated with load demand, real-time electricity price and wind power generation. A new robust solution using occupancy-based DR is presented in [24] under thermal comfort requirements with the energy storage and renewable energy sources. In [25], a new decision-making approach of DR for an energy consumer called "auction decision procedure" is proposed to help satisfy the DR in a decentralized manner. In [26], some packages of price strategy are offered for the implementation of DR to minimize operating costs and emissions considering uncertainties of wind and solar powers. In [27], a price-based DR is suggested to mitigate the difficulties of MG energy management in the presence of uncertainties of DG units and load demand. However, the time-based programs are not studied in it. In [28] a power management algorithm including DRP is presented for the multi-timescale operation of an islanded MG; while the grid-connected mode for the MG is not considered. Besides, the stochastic nature of the demand and DG units is not

studied.

In this paper, two principal categories of DRPs including incentive-based and time-based programs are applied to the operation of MG. Then the results obtained for six potential programs of two main types of DR (*i.e.* incentive-based DR including DLC, I/C, and EDRP as well as time-based programs including TOU, RTP and CPP) are extensively investigated. Moreover, uncertainties of some parameters of MG operation and also the possibility that the customers may not respond to DRPs are formulated. In summary, the contributions of this paper are as follows:

- To model different types of DRPs based on the price elasticity of demand and the customer benefit in the operation of MG.
- To solve the economic dispatch and unit commitment problem based on the AC power flow in the MG operation with the aim of minimizing the operation cost along with the implementation of different types of DRPs.
- To consider the random outages of transmission lines, the connection to the upstream grid and MTs as well as modeling uncertainties related to the load demand prediction, the forecasted power of wind and photovoltaic (PV) units.
- To model uncertainties related to the customer response in I/C program in the operation of MGs based on the Monte Carlo simulation.
- To provide a priority list of DRPs based on the weighting approach from the viewpoint of microgrid operator (MO) considering the effects of MG operation cost on the priority list.
- To consider grid-connected mode to exchange power between the MG and upstream grid.

The rest of the paper is organized as follows: Section 2 discusses different types of DRPs and their formulations. Details for the proposed modeling of PV and wind units in the operating mode of an MG for both cases of with/without the DRPs are provided in Section 3. In Section 4, case studies and results are presented. The paper is concluded in Section 5.

2 DEMAND RESPONSE MODELING

DR is the commitment of final customers in the electricity market which might be in respond to an hourly price change or an incentive program [29]. The DRPs investigated in this paper can be categorized into incentive-based programs and time-based rate programs [14]. Each of these programs can also be divided to several sub-sets. Three sub-sets of incentive-based programs include DLC, I/C and EDRP, and three sub-sets of time-based programs

include TOU, RTP and CPP.

Since the energy price is directly affected by demand and customers regulate their power consumption, to model the DR, the relation between energy price and demand in each time period should be modeled first. Therefore, the price elasticity of demand, *E*, as the sensitivity between the relative change in demand *q* and the relative change in price ρ is defined as follows [30]:

$$E = \frac{dq/q}{dr/r} = \frac{r}{q}.\frac{dq}{dr} \tag{1}$$

When the energy price is variable during different time periods, the load demand can be categorized into the following two groups [30]:

a) Loads which cannot be deferred during the considered time horizon and can only switch between on and off modes.

b) Controllable loads that can be deferred from peak to off-peak times when the load amount is moderate or low.

Small power consumers do not react to price changes easily and they can be considered as the first group. But large industrial customers tend to decrease their load in peak hours and shift it to off-peaks. Therefore, they are classified in the second group. The cross-elasticity between the demand of period *z* and the price of period $z^{'}$ can be formulated as:

$$Ezz' = \frac{dq_z/q_z}{dr_{z'}/r_{z'}} = \frac{r_{0z'}}{q_{0z}}.\frac{dq_z}{dr_{z'}} \tag{2}$$

Self-elasticity is always negative while cross elasticity is always positive.

2.1 MODELING OF SINGLE PERIOD ELASTIC LOADS

Initially, to make the system simpler, it is assumed that only one customer exists. Then, the obtained equations will be extended to a larger number of customers. The day is divided into multiple time periods based on the demand. If the demand and customer's income in the z^{th} period are represented by d_Z and B_z^0 respectively, the customer changes the load by Δd_Z when the customer receives $A_z(cent/kWh)$ or the energy price changes from r to r_z. Hence, the total profit of the customer in the z^{th} period after applying DRP is calculated by $A_z * \Delta d_z$.

The customer's income after applying DRP and change in demand is represented by B_z as calculated by (3) [18]

$$B_z = B_z^0 + r_{0z}\Delta d_z\left(1+\frac{\Delta d_z}{2E_{zz}d_z}\right) - A_z * \Delta d_z \tag{3}$$

where E_{zz} is the self-elasticity of z^{th} period and B_z is the customer's income after change in demand in the z^{th} period.

The earned profit of consuming energy by the customer can be calculated by (4) as follows:

$$S_z = B_z - r_z\left(d_z + \Delta d_z\right) = B_z^0 + r_{0z}\Delta d_z\left(1+\frac{\Delta d_z}{2E_{zz}d_z}\right) - A_z * \Delta d_z - r_z\left(d_z + \Delta d_z\right) \tag{4}$$

To maximize the customer's profit, the derivative of the profit function is set to be zero and the optimal Δd_z^* is solved as follows:

$$\frac{\partial S_z}{\partial \Delta d_z} = r_{0z} + r_{0z}\frac{\Delta d_z}{E_{zz}d_z} - A_z - r_z = 0 \tag{5}$$

Then:

$$\Delta d_z = E_{zz}d_z\frac{(A_z + r_z - r_{0z})}{r_{0z}} \tag{6}$$

Therefore, if the customer changes his/her load based on (6), the maximum profit will be earned. Since Δd_z in (6) is a negative value due to the negative self-elasticity term, it is denoted by Δd_z^- as in (7).

$$\Delta d_z^- = E_{zz}d_z\frac{(A_z + r_z - r_{0z})}{r_{0z}} \tag{7}$$

2.2 MODELING OF MULTI PERIOD ELASTIC LOADS

In this section, the possibility of shifting load to other periods is modeled by considering the cross elasticity. Load change due to shifting to other periods represented by Δd_z^+, is calculated by (8) in which $E_{zz'}$ shows the cross elasticity of z^{th} period to $(z')^{th}$ period.

$$\Delta d_z^+ = \sum_{z'=1, z'\neq z}^{NZ} E_{zz'}d_z\frac{(A_{z'} + r_{z'} - r_{0z'})}{r_{0z'}} \tag{8}$$

$$\frac{(A_{z'} + r_{z'} - r_{0z'})}{r_{0z'}} = \frac{\Delta d_{z'}^-}{E_{z'z'}d_{z'}} \tag{9}$$

Based on (9), the load which is deducted from other periods and shifted to the z^{th} period can be calculated by (10).

$$\Delta d_z^+ = \sum_{z'=1, z' \neq z}^{NZ} \frac{E_{zz'}}{E_{z'z'}} \frac{d_z}{d_{z'}} \Delta d_{z'}^- \tag{10}$$

2.3 FINAL MODEL

In the final model, this formulation will be extended by considering several customers for each hour under different scenarios. Then, by performing some simplifications and mathematical operations, the following equation is defined for different DRPs [18].

$$DR_{i,t,s}^- = P_{i,t,s}^D \left|E_{zz}\right| \frac{(A_{i,t} + r_t - r_{0t})}{r_{0t}} \quad if\ z \in Z_t \tag{11}$$

Equation (11) shows the amount of load change as the results of employing DR for bus *i* when the costumers accept this program. On the other hand, the I/C loads should be fined if they do not agree to perform the DRP. The $IC_{i,t,s}$ is indicative of the customer's response to I/C program; its value is 0 if customers ignore the DRP, and is 1 if customers accept the DRP. Moreover, in all DRPs, except for I/C, its value is fixed to 1. Therefore, the amount of shifted load considering I/C loads can be calculated by:

$$DR_{i,t,s}^- = P_{i,t,s}^D \left|E_{zz}\right| \frac{(A_{i,t} \times IC_{i,t,s} + r_t - r_{0t})}{r_{0t}} \quad if\ z \in Z_t \tag{12}$$

The value of penalty due to the refusal of load reduction is calculated by:

$$PC_{i,t,s}^{IC} = PP_{i,t} \times DR_{i,t,s}^- \times (1 - IC_{i,t,s}) \tag{13}$$

Customers' reward as the result of accepting the DRP is calculated by:

$$C_{i,t,s}^{DR} = A_{i,t} \times DR_{i,t,s}^- \times IC_{i,t,s} - PC_{i,t,s}^{IC} \tag{14}$$

The shifted load to an off-peak hour based on cross elasticity is calculated as follows:

$$DR_{i,t,s}^+ = \frac{P_{i,t,s}^D}{D_{i,z,s}} \sum_{z'=1, z' \neq z}^{NZ} \frac{E_{zz'}}{\left|E_{z'z'}\right|} \frac{D_{i,z,s}}{D_{i,z',s}} \left(\sum_{t' \in T_{z'}} DR_{i,t',s}^- \right) \quad if\ z \in Z_t \tag{15}$$

$$D_{i,z,s} = \sum_{t \in T_z} P_{i,t,s}^D \tag{16}$$

Therefore, the new amount of load $P_{i,t,s}^{D,Mod}$ after applying the DRP can be formulated by:

$$P_{i,t,s}^{D,Mod} = P_{i,t,s}^D + DR_{i,t,s}^+ - DR_{i,t,s}^- \tag{17}$$

3 DR MODELING IN MG OPERATION

The optimal operation of an up-grid connected MG including DGs is important for minimizing total cost of the

system. In these types of grids, the operator determines MG scheduling for one or more days ahead employing predicted powers of renewable generation units to minimize operating costs. DRPs are effective options in order to reduce the peak load and thereby reduce the operating costs in the critical moments.

3.1 WIND AND PV MODELING

Power generated from wind turbines depends on the hourly historical wind speed data collected annually over a significant period at the wind farm location. The evaluation process should also accurately model the intermittent nature of power output from the wind farm. Moreover, wind power studies require accurate models to forecast the wind speed variation at wind farm locations [31]. In general, wind speed probability distributions are often characterized by Weibull distributions. According to the shaping parameters, Weibull distribution in general can have different forms. When the wind speed probability distribution obtained from a real geographical location is close to normal distribution, wind speed distribution can be represented by Normal distribution [31]. In this paper, because of resemblance of wind speed probability distribution to normal distribution, wind distribution and its relevant error is characterized by the normal distribution. It has been proposed in some research that normal distribution functions can be proposed for modeling of the uncertainty of forecast in the estimation of load demand, wind power and solar energy [31,32, 33]; while mean value refers to the peak of the forecast. If a normal distribution is separated to several discrete intervals, the probability value corresponding to each interval can be estimated using linearization. In the case of wind turbines (WTs), the detailed equations for calculating the wind output power from the wind speed are illustrated by (18) to (21) [31].

$$P_t^w = \begin{cases} 0 & , \quad 0 \le SW_t < V_{ci} \\ \left(A + B \times SW_t + C \times SW_t^{\,2}\right) \times P_r & , \quad V_{ci} \le SW_t < V_r \\ P_r & , \quad V_r \le SW_t < V_{co} \\ 0 & , \quad SW_t \ge V_{co} \end{cases} \tag{18}$$

in which

$$A = \frac{1}{\left(V_{ci} - V_r\right)^2}\left\{V_{ci}\left(V_{ci} + V_r\right) - 4V_{ci}V_r\left[\frac{V_{ci} + V_r}{2V_r}\right]^3\right\}, \tag{19}$$

$$B = \frac{1}{\left(V_{ci} - V_r\right)^2}\left\{4\left(V_{ci} + V_r\right)\left[\frac{V_{ci} + V_r}{2V_r}\right]^3 - \left(3V_{ci} + V_r\right)\right\}, \tag{20}$$

$$C = \frac{1}{\left(V_{ci} - V_r\right)^2}\left\{2 - 4\left[\frac{V_{ci} + V_r}{2V_r}\right]^3\right\} \tag{21}$$

A nonlinear wind-power specification curve for these turbines is depicted in Fig. 1. Obviously, the generated power varies with the wind speed at the site of wind farm. The output power of wind generator can be determined using its generation power curve, which is a plot of the output power of turbine versus wind speed. A wind generator is designed to start generating power at the cut-in speed V_{ci} and shut down for safety reasons at the cut-out speed

V_{co}. The rated power P_r is generated when the wind speed is between the rated speed V_r and the cut-out speed V_{co}. There is a nonlinear relationship between the output power and the wind speed when the wind speed lies within the cut-in speed V_{ci} and the rated speed V_r. The annual mean μ and standard deviation σ for wind speed data and model at the site of wind farm are used for depicting the common wind speed model as shown in Fig. 82. This site-specific wind speed model is then combined with the wind generator power curve to obtain the wind turbine power generation model.

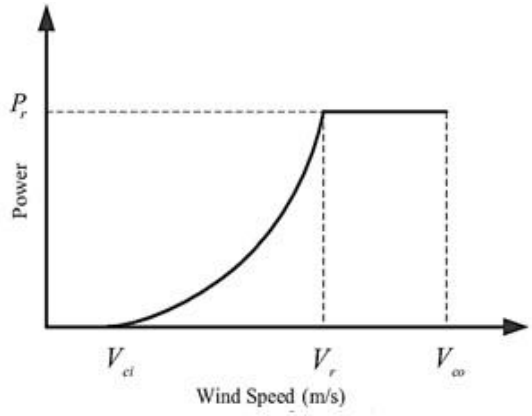

Fig. 1: Wind turbine power curve

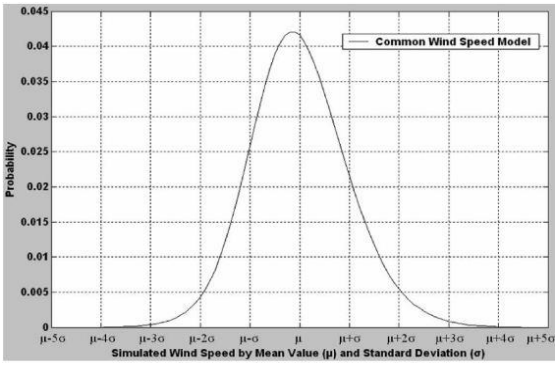

Fig. 2: Common wind speed model

In this paper, same as wind speed prediction, the solar radiation distribution is characterized by the normal distribution [31,34,35]. With prediction of solar radiation, the amount of power produced by the solar modules according to the type and size of solar cells is calculated by (22) [36].

$$P_{pv,t,s}^{PV} = h_{pv}^{PV} \times S_{pv}^{PV} \times f_{pv,t,s}^{PV} \tag{22}$$

3.2 DRPS MODELING IN MG OPERATION

The objective of the paper is to reduce hourly operating costs of MG which is expressed as follows [37]:

$$\begin{aligned} Cost = \sum_{s=1}^{NS} p_s \times \{ & \sum_{t=1}^{NT} \sum_{mt=1}^{Nmt} (a_{mt} u_{mt,t,s} + b_{mt} P_{mt,t,s}^{MT}) \\ & + \sum_{t=1}^{NT} \sum_{i=1}^{Ni} VOLL_{i,t} LS_{i,t,s} + \sum_{t=1}^{NT} \sum_{i \in IDR} C_{i,t,s}^{DR} \\ & + \sum_{t=1}^{NT} r_t P_{i,t,s}^{buy} - \sum_{t=1}^{NT} r_t P_{i,t,s}^{sell} \} \end{aligned} \tag{23}$$

Here, the first term refers to the total operation cost of MTs; while the second term shows the costs as the result of demands not to be supplied. The third term shows the financial transactions from selling and buying energy to/from the upstream. Equation (23) is used to minimize the cost of MG operation subjected to (24)-(40). Equations (24) and (25) refer to the load-balance constraint in order to maintain the frequency of MG within the permitted

range. Equations (26)-(28) show the power limit constraints of DGs (wind, PV and MT). Possibility of financial transactions with the upstream is limited due to security and facility obligations based on (29). Constraints related to the battery storage are detailed by (30) to (35).

$$\sum_{mt\in MT_i} P_{mt,t,s}^{MT} + \sum_{w\in W_i} P_{w,t,s}^{W} + \sum_{pv\in PV_i} P_{pv,t,s}^{PV} + \sum_{b\in Bat_i} P_{b,t,s}^{B} = \sum_{j\in Bus_i} PL_{i,j,t,s} + \left(P_{i,t,s}^{D} + DR_{i,t,s}^{+} - DR_{i,t,s}^{-} - LS_{i,t,s}\right) \quad \forall i \neq slack \tag{24}$$

$$\sum_{mt\in MT_i} P_{mt,t,s}^{MT} + \sum_{w\in W_i} P_{w,t,s}^{W} + \sum_{pv\in PV_i} P_{pv,t,s}^{PV} + \sum_{b\in Bat_i} P_{b,t,s}^{B} + \left(P_{i,t,s}^{buy} - P_{i,t,s}^{sell}\right) = \sum_{j\in Bus_i} PL_{i,j,t,s} + \left(P_{i,t,s}^{D} + DR_{i,t,s}^{+} - DR_{i,t,s}^{-} - LS_{i,t,s}\right) \quad \forall i = slack \tag{25}$$

$$P_{mt}^{MT,\min} \times u_{mt,t,s} \le P_{mt,t,s}^{MT} \le P_{mt}^{MT,\max} \times u_{mt,t,s} \tag{26}$$

$$P_{w,t,s}^{W} \le P_{w,t,s}^{W,forecast} \tag{27}$$

$$P_{pv,t,s}^{PV} \le P_{pv,t,s}^{PV,forecast} \tag{28}$$

$$P_{i,t,s}^{buy} \le P^{Grid,\max} \times u_{t,s}^{Grid},\ P_{i,t,s}^{sell} \le P^{Grid,\max} \times \left(1 - u_{t,s}^{Grid}\right) \tag{29}$$

$$P_{b,t,s}^{B} = P_{b,t,s}^{dc} - P_{b,t,s}^{ch} \tag{30}$$

$$P_{b}^{ch,\min} \times u_{b,t,s}^{ch} \le P_{b,t,s}^{ch} \le P_{b}^{ch,\max} \times u_{b,t,s}^{ch} \tag{31}$$

$$P_{b}^{dc,\min} \times u_{b,t,s}^{dc} \le P_{b,t,s}^{dc} \le P_{b}^{dc,\max} \times u_{b,t,s}^{dc} \tag{32}$$

$$u_{b,t,s}^{ch} + u_{b,t,s}^{dc} \le 1 \tag{33}$$

$$E_{b,t,s}^{B} = E_{b,(t-1),s}^{B} + h_{b}^{ch} \cdot P_{b,t,s}^{ch} - \frac{1}{h_{b}^{dc}} P_{b,t,s}^{dc} \tag{34}$$

$$E_{b}^{B,\min} \le E_{b,t,s}^{B} \le E_{b}^{B,\max} \tag{35}$$

where Bus_i, Bat_i, PV_i, W_i and MT_i are the sets of buses, batteries, solar units, wind units and MTs connected to bus i respectively. In (34), the time interval is considered one hour. In this paper, the AC power flow is utilized. The power flow of lines is limited based on (36) to (40).

$$PL_{i,j,t,s} = G_{i,j}\left|V_{i,t,s}\right|^2 - \left|V_{i,t,s}\right|\left|V_{j,t,s}\right|\left\{G_{i,j}\cos\left(d_{i,t,s} - d_{j,t,s}\right) + B_{i,j}\sin\left(d_{i,t,s} - d_{j,t,s}\right)\right\} \tag{36}$$

$$QL_{i,j,t,s} = -B_{i,j}\left|V_{i,t,s}\right|^2 - \left|V_{i,t,s}\right|\left|V_{j,t,s}\right|\left\{G_{i,j}\sin\left(d_{i,t,s} - d_{j,t,s}\right) - B_{i,j}\cos\left(d_{i,t,s} - d_{j,t,s}\right)\right\} \tag{37}$$

$$-SL_{i,j}^{\max} \le \sqrt{PL_{i,j,t,s}^2 + QL_{i,j,t,s}^2} \le SL_{i,j}^{\max} \tag{38}$$

$$V_i^{\min} \le V_{i,t,s} \le V_i^{\max} \tag{39}$$

$$\begin{cases} V_{i,t,s} = 1 \\ d_{i,t,s} = 0 \end{cases} \quad \forall i = slack \tag{40}$$

Diagram of the simulation procedures is depicted in Fig. 3. Assessment of the proposed methodology is conducted based on the simulation and results provided in Section 4.

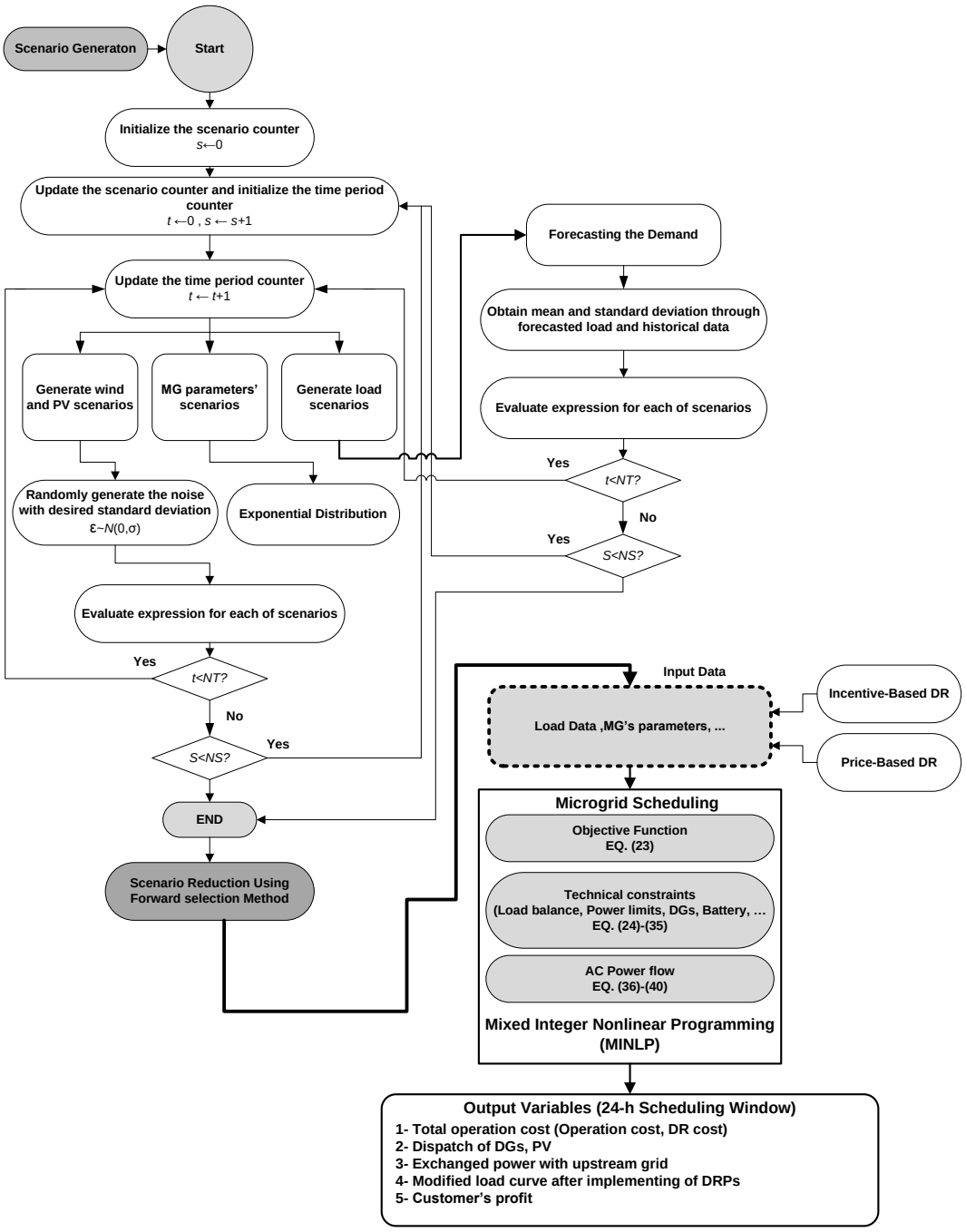

Fig. 3: Diagram of the simulation procedures

4 CASE STUDIES AND RESULTS

In this paper, different types of DRPs are modeled in operation of MGs. Different scenarios are simulated for each case to model MG uncertainties including failure of generation units and transmission lines, accessibility to the upstream grid, load forecasting error, error in the power prediction of DGs (wind and solar) and the declining probability to DRP from the interruptible load. Monte Carlo simulation is utilized for scenarios generation, and then scenario reduction method is applied to minimize the computational burden of the problem at a suitable level of accuracy. The methodology is applied on an 11-bus MG for a 24-hour period [38] and a 14-bus system for a 336-hour (two-week) scheduling horizon [39] . These problems are modeled as mixed-integer nonlinear programming (MINLP) problems which can be solved under the GAMS optimization software on an Intel(R) Core(TM) i7-Q740 @ 1.73GHz, RAM 4GB system [40].

4.1 FIRST CASE STUDY: 11-BUS MICROGRID

Fig. 4 shows the single line diagram of 11-bus MG. The configuration data related to this MG is detailed in [35] and [38]. The MG includes two MTs, one WT, one PV and one battery.

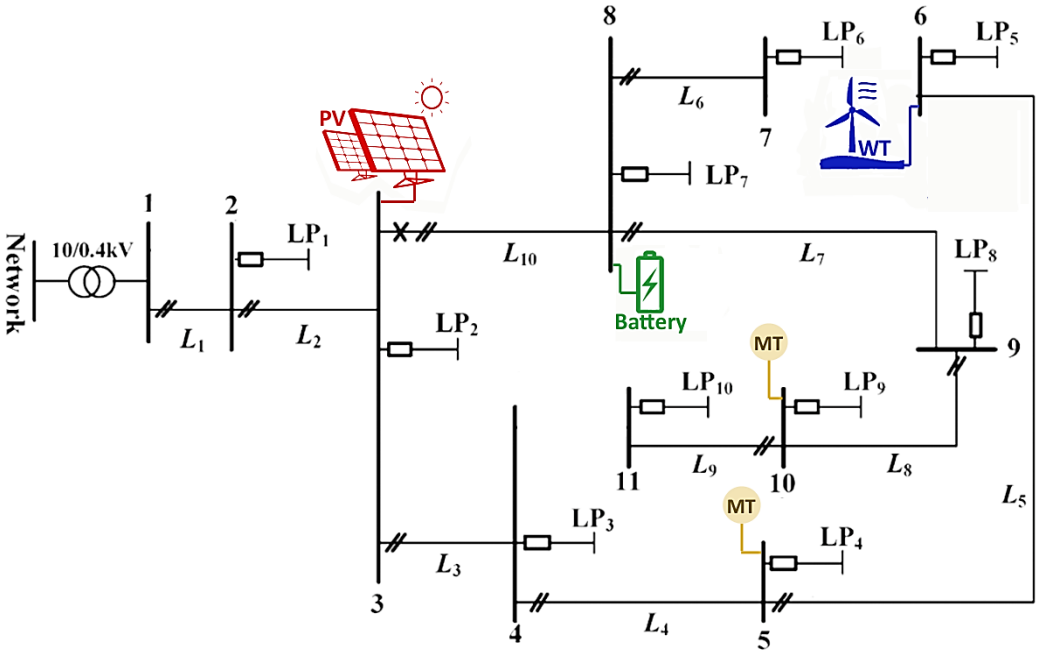

Fig. 4: 11-bus microgrid

The capacity of wind unit located at bus 6 is 15 kW; while the capacity of PV located at bus 3 is 25 kW. The specific model and specifications of the PV cell used in this paper are presented in [41]. Based on the model presented in Section 3.1, the forecasted power of wind and PV units are depicted in Fig. 5 in per unit of their corresponding maximum capacity [35, 38].

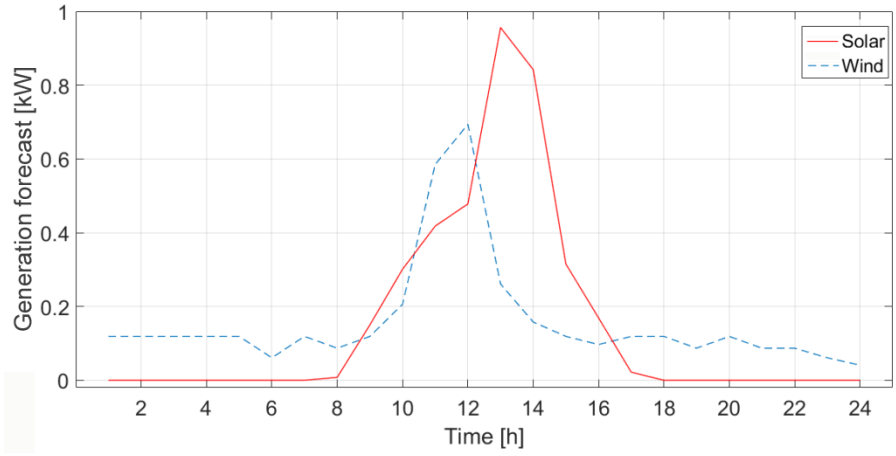

Fig. 5: Forecasted generation of wind and PV units for 11-bus MG

A battery storage unit is considered in this MG. The maximum accessible capacity of this unit for operation of MG is 30 kWh; while the minimum charge and discharge rates are 15 kW. The initial state of the battery is considered to be 20 kWh. The battery unit is located at bus 8 [35,38]. Per-unit hourly prediction of the load demand with the peak of 90 kW is shown in Fig. 6 [38].

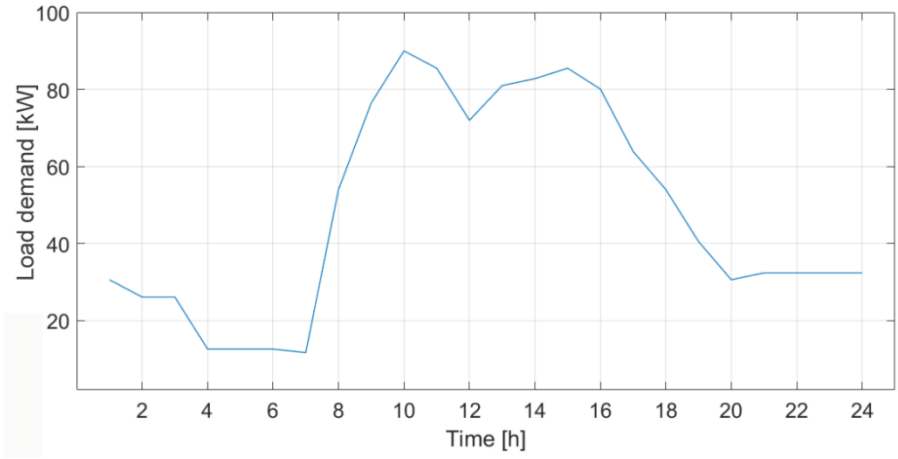

Fig. 6: Per-unit hourly prediction of load demand

The load ratio for each of the buses is considered as same as that in [38]. A medium-voltage system with the capacity of 100 kVA is designed as the upstream grid which provides 80% of its capacity due to operating constraints. The hourly price of selling and purchasing energy from upstream is depicted in Fig. 7 [35].

In this paper, it is considered that 20% of the demand participates in DRP. The price elasticity of the demand is given in Table 1 [21] and data related to the failure probability of transmission lines, MTs and the upstream grid is based on [38]. In this study, based on some papers, the simulated load demand scenarios are assumed to follow a normal distribution with a standard deviation of 5% of expected values which are the forecasted values given in Fig. 6. In addition, the standard deviation of expected values for wind power and solar power scenarios is 10% [32].

Ideally, it may be assumed that all costumers respond to the DRP; however in the real circumstances, the

costumer can dismiss the operator's request, or in terms of equipment, it is not possible to shed the load. In this regard, the customer's probability of ignoring the DRP is assumed as 10%. It should be mentioned that the value considered for this parameter is selected based on the operator's needs. Lower values of this parameter refer to the higher effect of DRP on the network operation.

The penalty cost of load shedding is considered to be 400 cents/ kWh. Scenario generation for uncertainties associated with the desired parameters is modeled by Monte Carlo simulation, in which 1000 scenarios generated for each of parameters are reduced to 8 as detailed in Table 2.

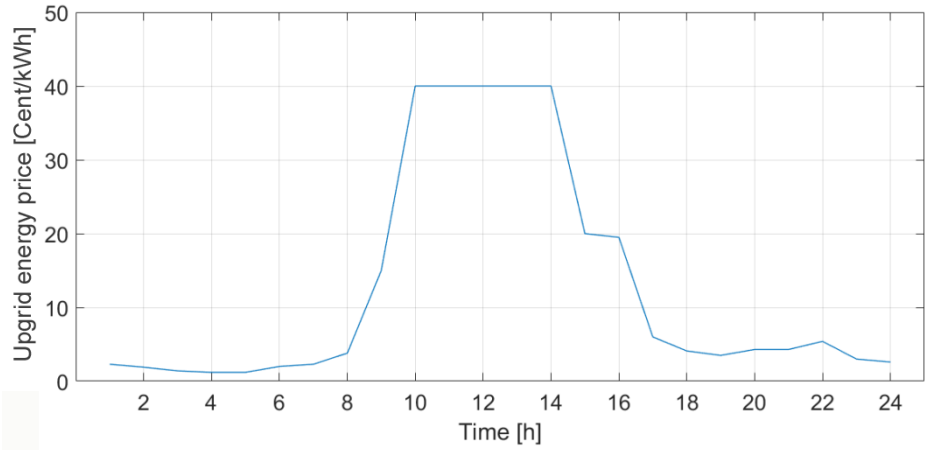

Fig. 7: Hourly price of selling and purchasing energy from upstream

Table 1: Self and cross elasticity factors in the 11-bus MG

	Low load	**Middle load**	**Peak**
Low load	-0.1	0.032	0.024
Middle load	0.032	-0.1	0.02
Peak	0.024	0.02	-0.1

The generated scenarios with low probability are removed or merged with those which are close to them to decrease the cost and time of investigating all possible states. Two major scenario reduction methods are Backward Reduction and Forward Reduction. SENERD option in GAMS software which is a Forward Reduction based method is employed in this research [40,42].

Table 2: The probability corresponding to each scenario in the 11-bus MG

Scenario #	**1**	**2**	**3**	**4**	**5**	**6**	**7**	**8**
Probability	0.168	0.189	0.079	0.107	0.106	0.089	0.148	0.114

The first step for modeling a stochastic program is modeling all the uncertainties in the problem. Normal distribution function is a common model for the uncertainty of forecast in the estimation of load demand, wind

power and solar energy. This normal distribution curve for seven intervals is depicted in Fig. 8. The second step for modeling the uncertainties is scenario generation.

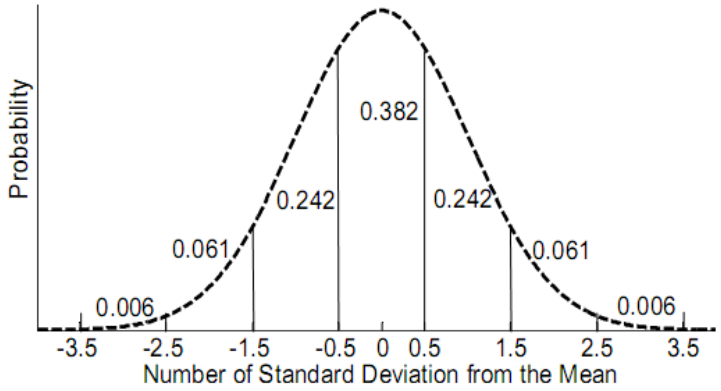

Fig. 8: Normal distribution

Scenario generation for the hourly load demand, wind power and solar generation are as follows:

1. Consider d_t^0 as the hourly forecasted value.
2. Consider $t = 1$, where t refers to the hour index.
3. Consider $s = 1$, where s refers to the scenario index.
4. Firstly, consider σ as the forecasting error or standard deviation of normal distribution function, and then generate a random number ψ_t^s based on a normal distribution function with mean value of d_t^0 and standard deviation of σ.
5. Calculate $d_t^s = d_t^0 + \psi_t^s * \sigma$.
6. Go to step 7 if all the required scenarios are generated; otherwise, $s = s + 1$ and go to step 4.
7. Go to step 8 if all the required hours are generated; otherwise, $t = t + 1$ and go to step 4.
8. Save all the generated scenarios, and end.

4.1.1 CASE 1: WITHOUT DRP

In this case, the simulation is implemented without DRP aiming at minimizing the operating costs of MG. The operating cost of MG and energy consumption for this case are 10895 cents and 10.28 kWh, respectively. As seen in Fig. 9, local DGs are not committed during scheduling hours in which the energy price in the upstream is low, and therefore loads are supplied by the upstream grid. Moreover, these hours are suitable for charging of batteries (i.e. orange curve). However, in case of hours with the high energy price, the operator tends to utilize DGs at their most capacity to have an opportunity of selling power to the upstream grid and subsequently achieve a considerable

profit (i.e. pink curve). During these hours, the battery unit is mostly discharging and MT generates at about its maximum capacity. For hours (after 18) in which the cost of energy generation by DGs and cost of purchasing power from upstream grid are approximately in the same range, the operator sets a trade-off between power produced by the upstream grid and local DGs; loads are supplied by both of these sources, and therefore there is no need for the highlighted commitment of local DG units.

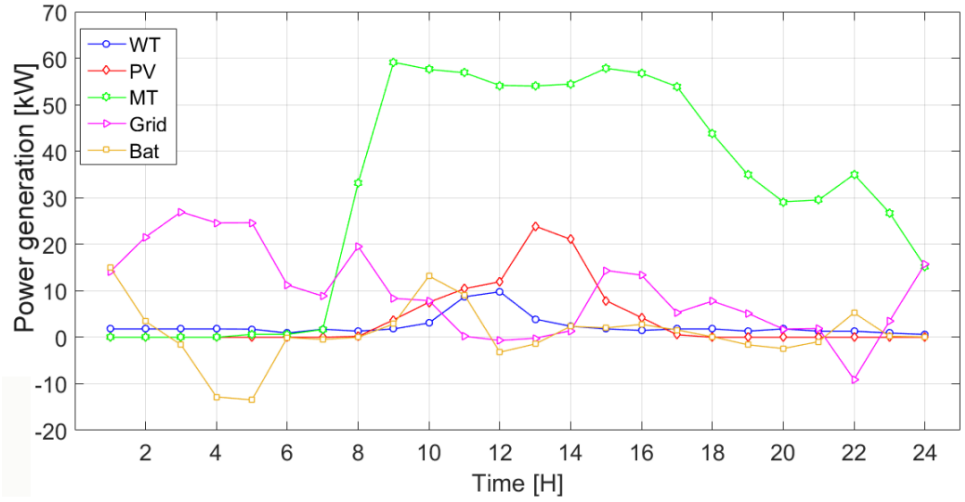

Fig. 9: Power generation of DGs and upstream grid in the case of 11-bus MG without DR

4.1.2 CASE 2: IMPLEMENTING DLC PROGRAM

In this scenario, the MG operator settles a DLC contract with customers to pay 20 cents/kWh for the reduction of load demand. In fact, the customer shifts this demand to another hour. The total cost for this scenario is 10102 cents, in which 9915 cents is related to the operation and 187 cents pertains to the implementation of DRP. The shaved curve of load demand as the implementation result of the DRP is depicted in Fig. 10. The load demand between hours 10 to 14 is reduced by 8.85 kWh due to the implementation of the DRP and paying the incentives. Moreover, 1.92 kWh is shifted to other hours due to cross elasticity.

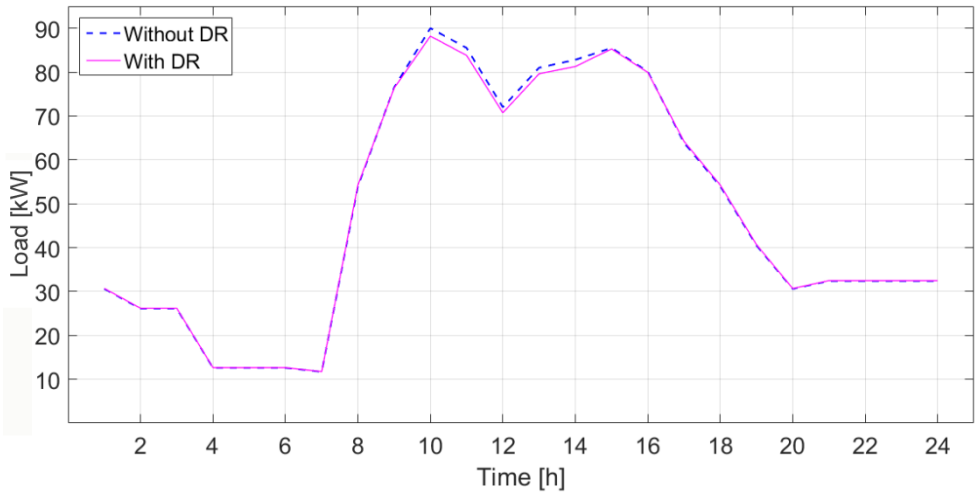

Fig. 10: Shaved curve of load after DLC implementation on the 11-bus MG

4.1.3 CASE 3: IMPLEMENTING I/C PROGRAM

In this scenario, as same as DLC, the MG operator settles a DLC contract with the customers to pay 20 cents/kWh for the reduction of the load demand; while there is a 40 cents/kWh penalty for customers who are not responding to the load reduction. The total cost for this scenario is 10140 cents, in which 9967 cents is related to the operation and 173 cents pertains to the implementation of DRP.

As seen in Fig. 11, the load demand between hours 9 to 16 is reduced by 8.27 kWh due to the implementation of the DRP and paying the incentives. Moreover, 1.83 kWh is shifted to other hours due to cross elasticity.

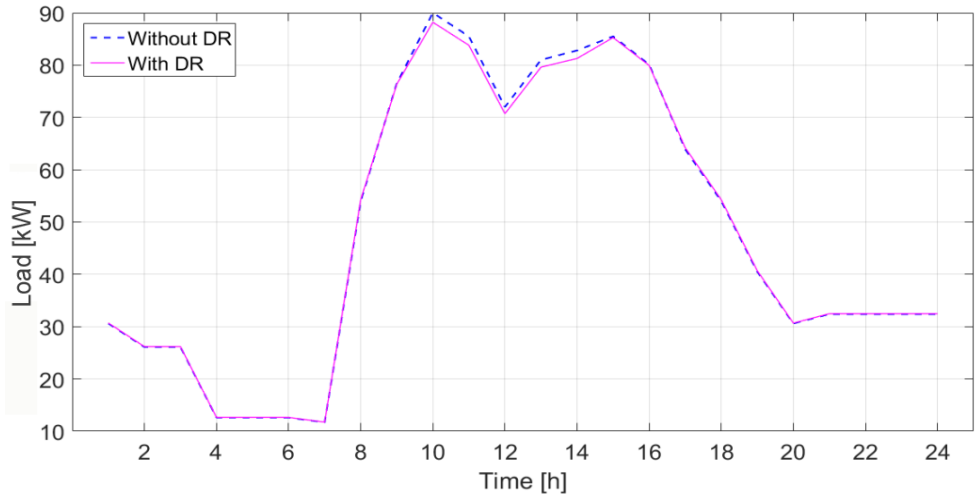

Fig. 11: Shaved curve of load after I/C implementation on the 11-bus MG

4.1.4 CASE 4: IMPLEMENTING EDRP

Implementation of EDRP pertains to situations in which a contingency occurs (*e.g.* outage of a line or generating unit). Therefore, the incentive value for this case is eye-catching in comparison with the previous cases. In such a way, the operator prevents a high amount of penalties as the result of loads not supplied. The value of incentive for this case is approximately considered to be five to ten times of the energy price in the MG (i.e. 120 cents/kWh for this study). The total operation cost for this case is 9845 cents, in which 9238 cents is related to the operation and 607 cents pertains to implementation of the EDRP. As it can be seen in Fig. 12, the load demand between hours 9 to 16 is reduced by 3.42 kWh due to the implementation of EDRP and paying the incentives. Moreover, 0.51 kWh is shifted to other hours due to the cross elasticity.

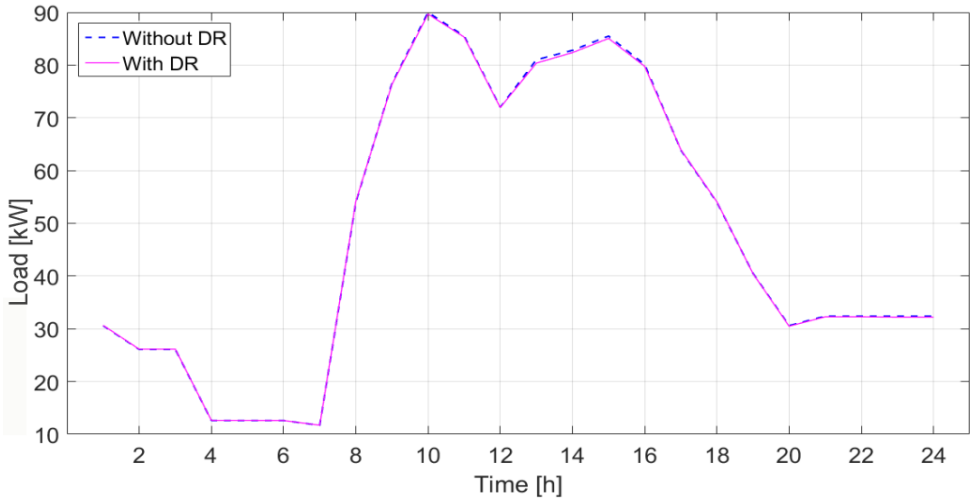

Fig. 12. Shaved curve of load after EDRP implementation on the 11-bus MG

4.1.5 CASE 5: IMPLEMENTING TOU PROGRAM

In this case, the single tariff stated in the previous cases is changed to a stepwise tariff in three periods corresponding to the load demand in three levels of low, medium and peak. In this research, the tariff for low, medium and peak loads are 5 cents/kWh, 20 cents/kWh and 40 cents/kWh, respectively. The total cost for this case is 9542 cents which is related to the operation; while there is no cost for implementation of the DRP.

The modified load demand profile after implementation of the DRP is depicted in Fig. 13. As seen, the load demand between hours 9 to 16 is reduced by 23.14 kWh due to the implementation of DRP and the electricity price in three zones; also, 7.87 kWh is shifted to other hours due to the cross elasticity.

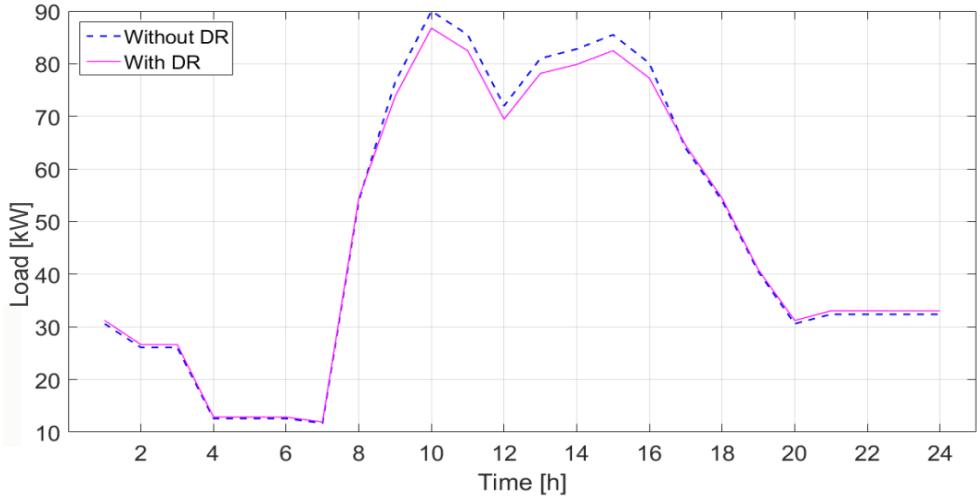

Fig. 13. Shaved curve of load after TOU implementation on the 11-bus MG

In order to reach a better realization of the operating cost reduction in running the TOU program comparing to the base case (without considering DRPs), the power dispatch for generating units of MG is shown in Fig. 14.

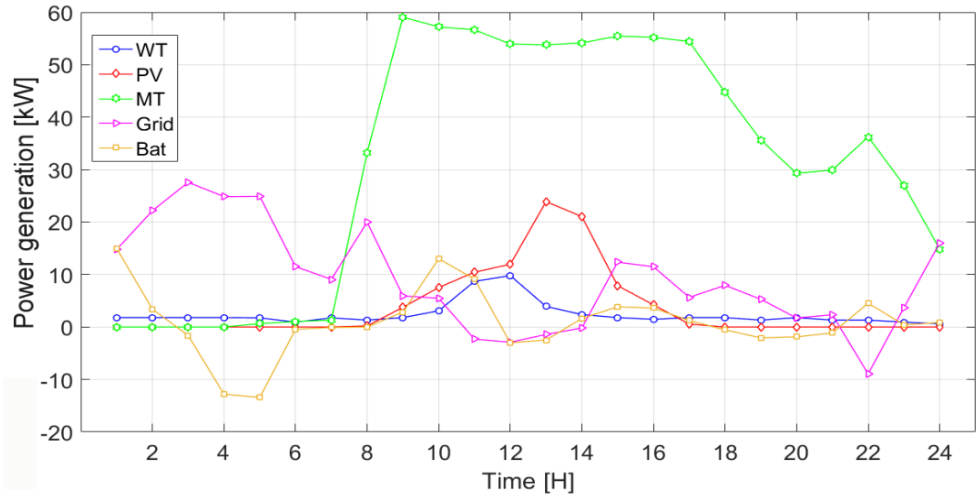

Fig. 14: Power dispatch after TOU implementation on the 11-bus MG

It can be seen that in this case, the customers give the grid operator the opportunity of selling power to the upstream grid and subsequent reduction of operating costs in addition to the demand-supply by the utilization of local generating units. The MT is not committed with its maximum capacity during peak hours (green curve) due to the failure probability in some scenarios.

4.1.6 CASE 6: IMPLEMENTING RTP PROGRAM

In this case, the electricity tariff is considered to be same as the price of purchasing power from the upstream grid. The total operating cost for this case is 9770 cents which is related to the operation; while, there is no cost for the implementation of DRP, which is same as other time-based DRP. The reshaped load curve after implementation of the load demand program is shown in Fig. 15. It can be seen that the load demand between hours 9 to 16 is reduced by 18.55 kWh due to the implementation of DRP. Moreover, 8.45 kWh is shifted to other hours due to cross elasticity.

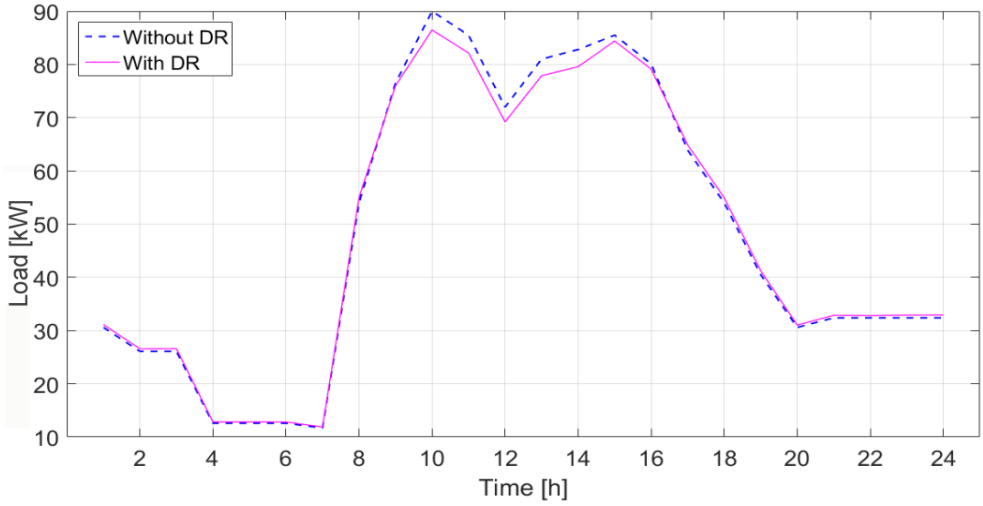

Fig. 15. Shaved curve of load after RTP implementation on the 11-bus MG

4.1.7 CASE 7: IMPLEMENTING CPP PROGRAM

This type of DR is utilized when a sudden demand increase happens. In such situations, customers corresponding to the increase of electricity tariff will decrease their demand. The electricity tariff is 200 cents/kWh between hours 10 to 15 for this MG. The total operation cost for this case is 8995 cents which is related to the operation; while, there is no cost for the implementation of DRP. The modified profile of load demand after the implementation of DRP is depicted in Fig. 16. As seen, the load demand between hours 10 to 15 is reduced by 42.31 kWh due to the implementation of DRP. Moreover, 10.07 kWh is shifted to other hours due to cross elasticity.

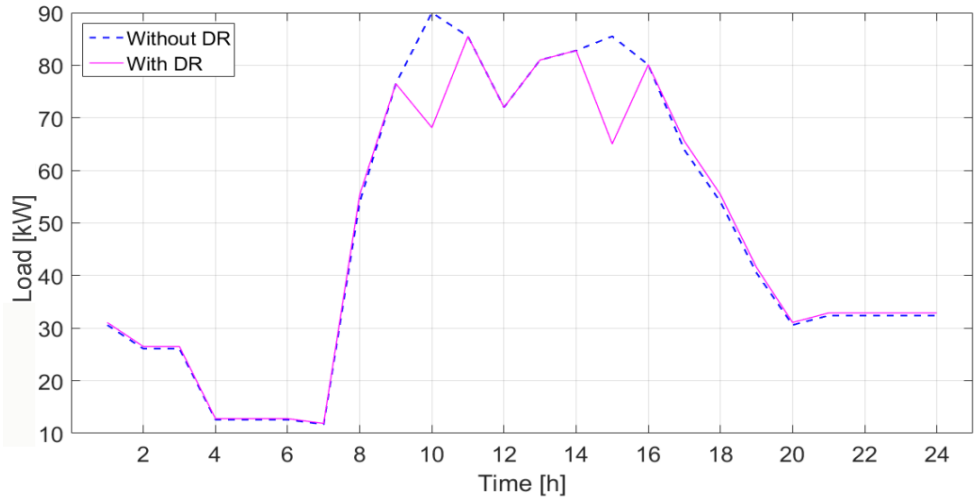

Fig. 16. Shaved curve of load after CPP implementation on the 11-bus MG

4.1.8 COMPARISON OF DRPS

This section aims to analyze the results obtained from the previous cases and compare them utilizing some indices which are appropriate for this obligation. The results detailed in Table 3 show that each of these DRPs has some superiorities in case of some indices.

Table 3: Detailed results obtained from implementing different types of DRPs in the 11-bus MG

DRP	Base case	DLC	I/C	EDRP	TOU	RTP	CPP
Penalty for refusing Load reduction (cent)	0	0	23	0	0	0	0
Peak reduction (kW)	0	1.9	1.8	0.327	3.2	3.5	4.5
Load factor (%)	53.6	54.5	54.4	53.7	54.9	55.3	54.9
Peak to valley (kW)	78.3	76.3	76.5	78	74.8	74.6	73.6
Energy reduction (kWh)	0	6.9	6.4	2.9	15.3	10.1	32.3
Energy consumption (kWh)	10.28	10.48	10.46	10.31	10.64	10.74	10.72

The total cost of operation including MG operation cost and DR cost is presented in Fig. 17. Moreover, the customer's profits for different cases are depicted in Fig. 18. Obviously, I/C program has the highest operating cost

and EDRP has the highest DR cost. As seen, CPP has the lowest operation cost, while the customers suffer from the greatest loss. On the other side, the EDRP with the highest profit for customers and an acceptable operation cost seems to be the best choice; however, as it can be seen in Fig. 19 and Table 3, it ranks lower in term of peak reduction etc. To this end, the TOU program seems to have a good rank on the priority list because of its acceptable performance regarding peak reduction and load factor. In order to better evaluate each case, the four best DRPs are sorted based on each of indices in Table 4.

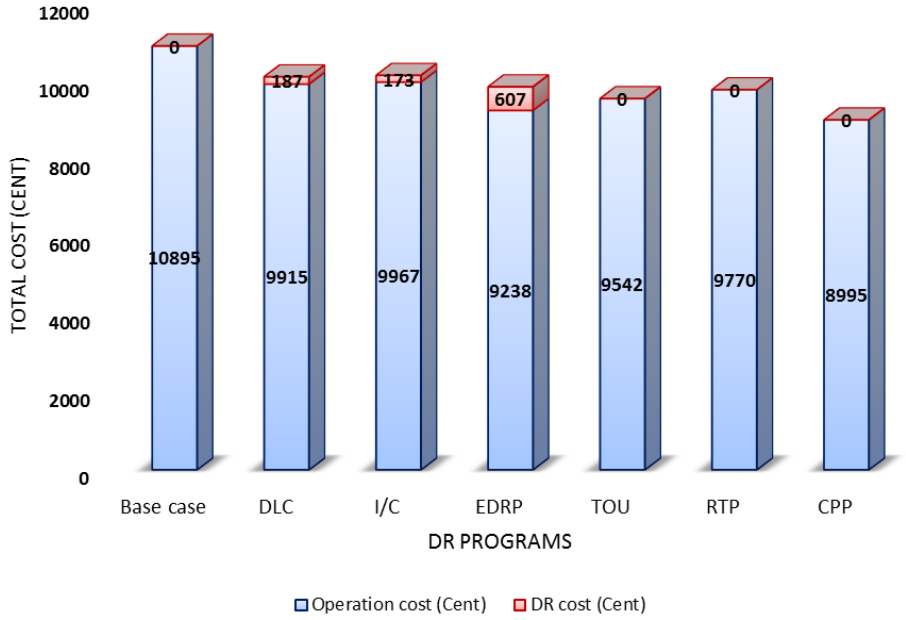

Fig. 17: Total operation cost including MG operation cost and DR cost for different DRPs in the 11-bus MG

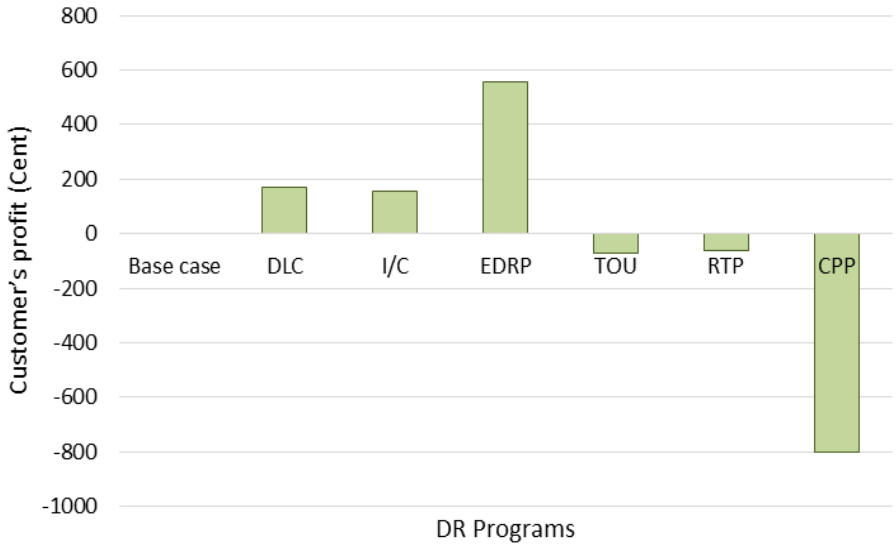

Fig. 18: Customer's profit for different DRPs in the 11-bus MG

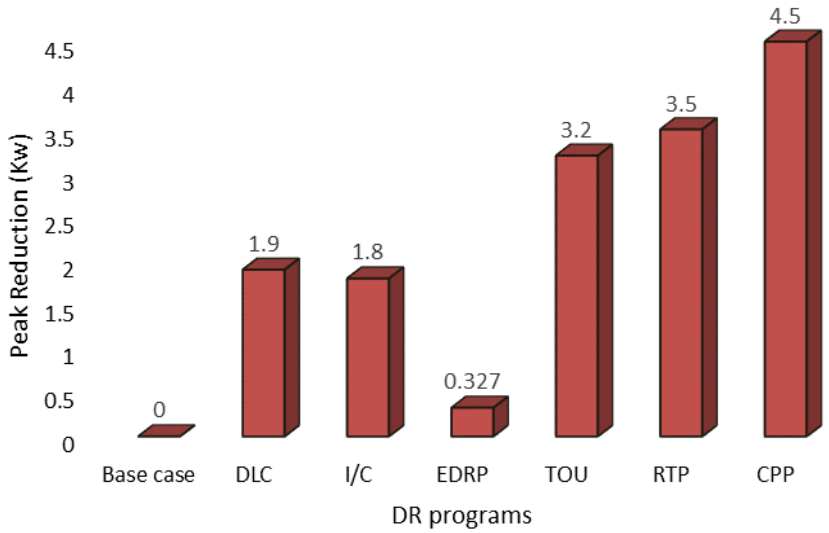

Fig. 19: Peak reduction for different DRPs in the 11-bus MG

Table 4: Ranking of DRPs for the 11-bus MG

Ranking	Rank 1	Rank 2	Rank 3	Rank 4
Total cost (cent)	CPP	TOU	RTP	EDRP
Customer's profit (cent)	EDRP	DLC	I/C	RTP
Peak reduction (kW)	CPP	RTP	TOU	DLC
Load factor (%)	RTP	CPP	TOU	DLC
Peak to valley (kW)	CPP	RTP	TOU	DLC
Energy reduction (kWh)	CPP	TOU	RTP	DLC
Energy consumption (kWh)	EDRP	I/C	DLC	TOU

Based on Table 4, the CPP has the best rank in terms of four indices; while it ranks last in terms of the important index of customers' profit. The RTP has the first rank in terms of load factor index, the second rank in terms of peak reduction and the third rank in terms of the total cost and energy reduction. Obviously, it is a hard challenge to find the best approach among these DRPs for an MG. A technique based on the weighting of indices is presented in [21]. Considering the given weights in Table 5 [21], the ranking of DRPs is shown in Fig. 20. It can be deduced that the EDRP is the best option when a contingency occurs or the level of uncertainties is high. The DLC and I/C seem to provide similar performances as the next options, and then the RTP and TOU have the next ranks. CPP which is the best regarding number of first-rank in Table 4 ranks the last due to its high expense for the customers.

Table 5: Weights of attributes

Index	Total Cost	Customer's profit	Peak reduction	Load factor	Peak to valley	Energy reduction	Energy consumption
Weight	0.393	0.393	0.062	0.023	0.051	0.023	0.055

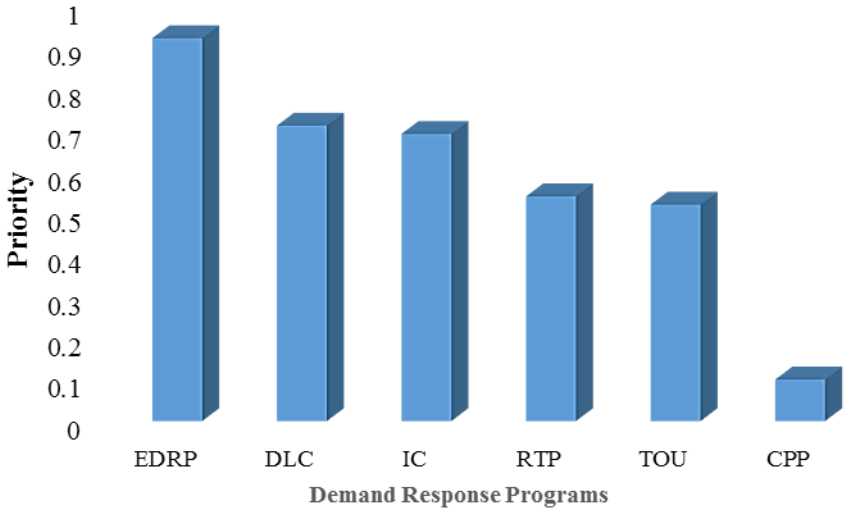

Fig. 20: Ranking of different DRPs for the 11-bus MG

4.2 SECOND CASE STUDY: 14-BUS MICROGRID

The configuration of 14-bus MG is shown in Fig. 21. The data related to this case study is given in [42]. The scheduling period is considered to be two weeks (*i.e.* 336 hours). This MG includes two MT units, four WT units, 10 PV units and one battery bank. The data related to MT units are provided in [39].

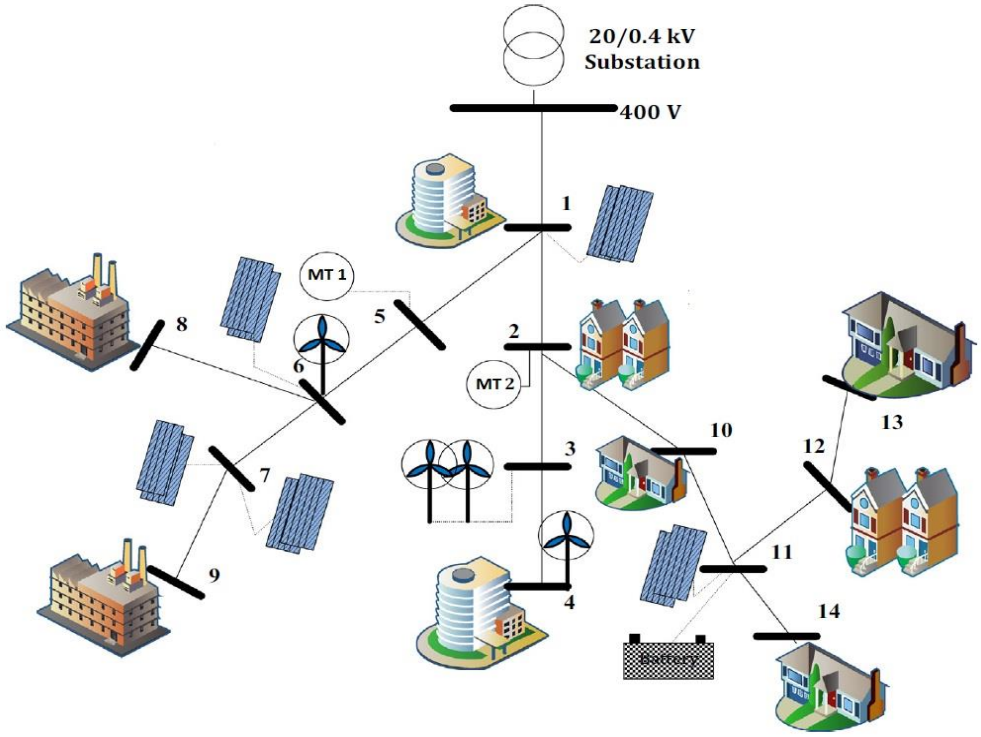

Fig. 21: Configuration of the 14-bus MG

The capacities of WT units located at buses 3, 6 and 4 are 30 kW; two WT units are installed at bus 3. As shown in Fig. 21, ten PV units with the capacity of 20 kW for each are divided to five equal sections and allocated to some buses of MG. The wind power prediction is shown in Fig. 22 [43]. The area of each PV unit is 40 m^2 [39].

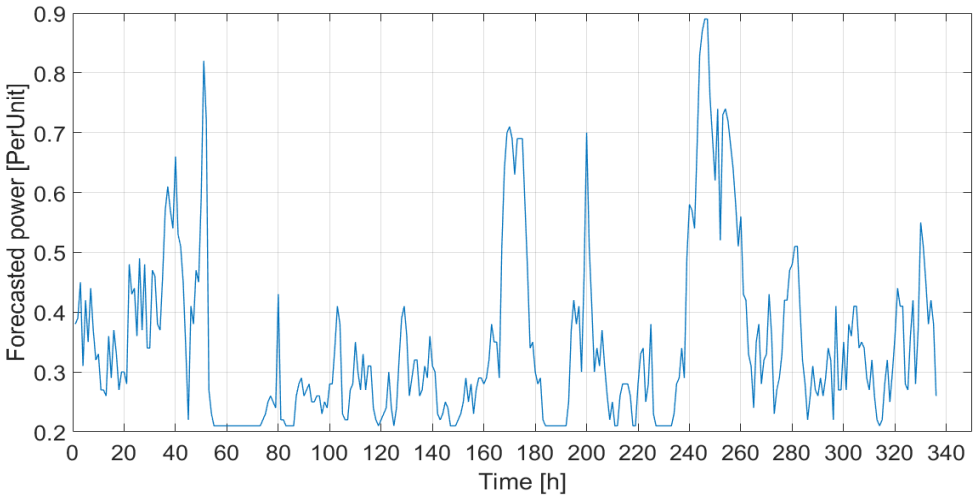

Fig. 22: Power forecasting of WT units in the 14-bus MG

In this MG, a battery with available operation capacity of 30 kWh, the minimum charge/discharge rate of 15 kW and the initial capacity of 12 kWh at bus 11 is considered. The load demand profile for this case study with the peak of 750 kW (per unit of peak load) is shown in Fig. 23 [44]. The ratios corresponding to the share of load for each bus are provided in [39].

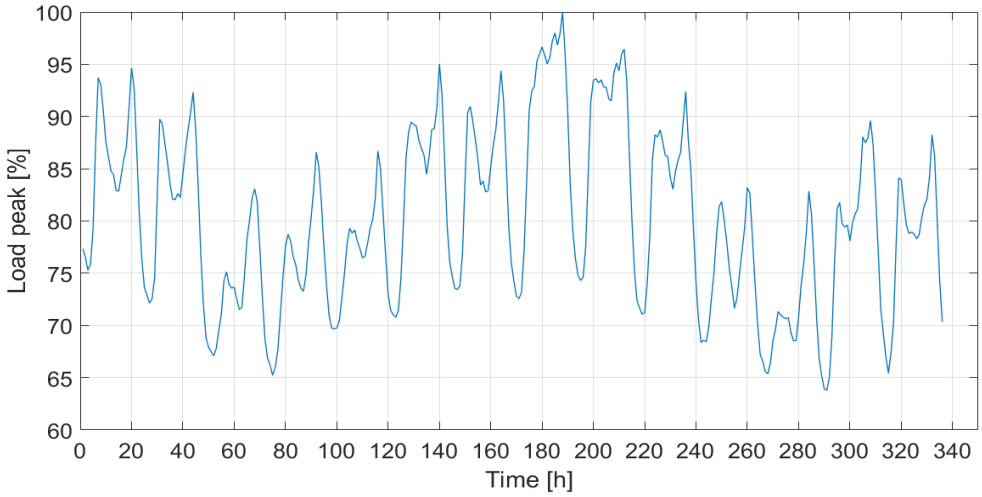

Fig. 23: Hourly load demand prediction for the 14-bus MG

The upstream grid is composed of a medium-voltage substation with the capacity of 1000 kVA where 80% of its capacity is accessible due to the operating limitations. Hourly prices of the selling and purchasing energy to/from the upstream are detailed in [44]. In this paper, it is considered that 20% of customers participate in the DRP. The price elasticity of demand is given in Table 6 [21]. Considering the load profile, hours 1-5 and 23-24 refer the low period, hours 6, 9-18 and 22 are the middle period, and hours 7-8 and 19-21 are the peak period. A single tariff is defined for the energy price in the MG as 10 cents/ kWh. The penalty corresponding to loads not supplied is 120 cents/kWh.

The uncertainties pertain to the failure of MT units and transmission lines, accessibility of upstream line, error

in load demand forecasting, error in the production of renewable energies (wind and solar) based DG units, and the possibility that customers ignore the load curtailment.

Table 6: Self and cross elasticity factors in the 14-bus MG

	Low load	**Middle load**	**Peak**
Low load	-0.1	0.032	0.024
Middle load	0.032	-0.1	0.02
Peak	0.024	0.02	-0.1

As described in the first case study, load prediction error (standard deviation), power forecasting error for wind and solar generation units, and possibility that customers do not respond to the programmed shedding are considered as 5%, 10% and 10%, respectively. The uncertainties are modeled by scenario generation and scenario reduction methods. In this case, after generation of 1000 scenarios, they are reduced to 8 scenarios. The probabilities corresponding to each of scenarios are provided in Table 7.

Table 7: Probability of each scenario for the 14-bus MG

Scenario#	**1**	**2**	**3**	**4**	**5**	**6**	**7**	**8**
Probability	0.164	0.071	0.096	0.093	0.085	0.086	0.081	0.324

Simulations of the MG are implemented for seven operating conditions (*i.e.* one base case and six DRPs). The results are detailed in Table 8.

Table 8: Simulation results for the 14-bus MG

DRP	**Base case**	**DLC**	**I/C**	**EDRP**	**TOU**	**RTP**	**CPP**
Penalty for refusing Load reduction (cent)	0	0	2161	0	0	0	0
Load factor (%)	80.2	79.6	79.6	79.2	81.7	79.2	80
Peak to valley (kW)	271.4	277.8	277.5	296.2	249.7	317	272.9
Energy reduction (kWh)	0	738.2	673	437.2	64.5	926.5	87
Energy consumption (kWh)	1352.3	1352.6	1353.1	1352.6	1355.24	1330.9	1353.2

The total cost of operation consisting of MG operation cost and DR implementation cost is shown in Fig. 24. The customer's profit for different cases is depicted in Fig. 25. It can be seen, same as the previous case studies, the RTP has the lowest cost of operation while it incurs the maximum cost for customers.

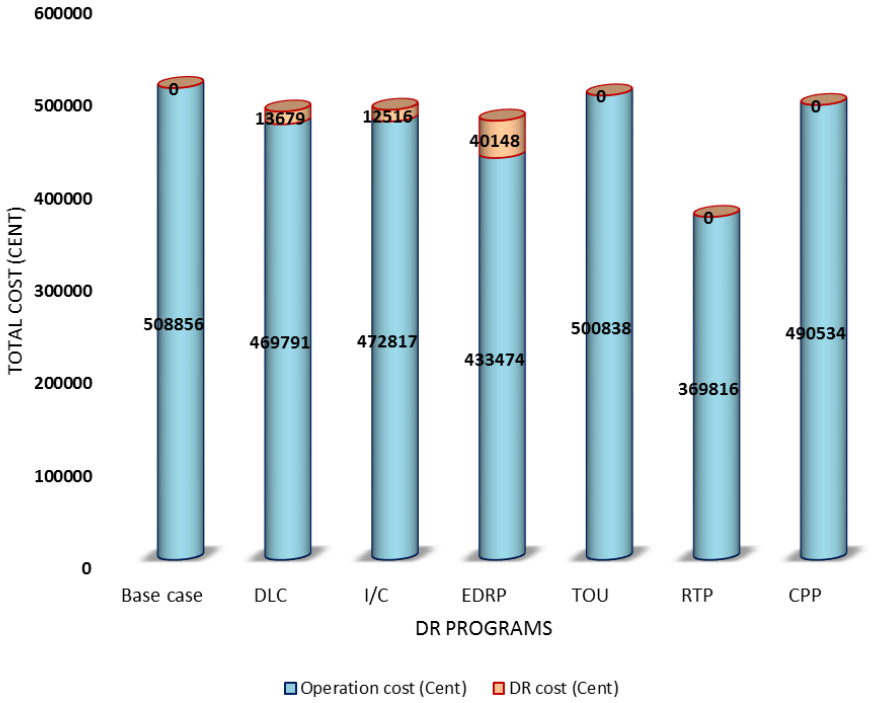

Fig. 24: Total operation cost including MG operation cost and DR cost for different DRPs in the 14-bus MG

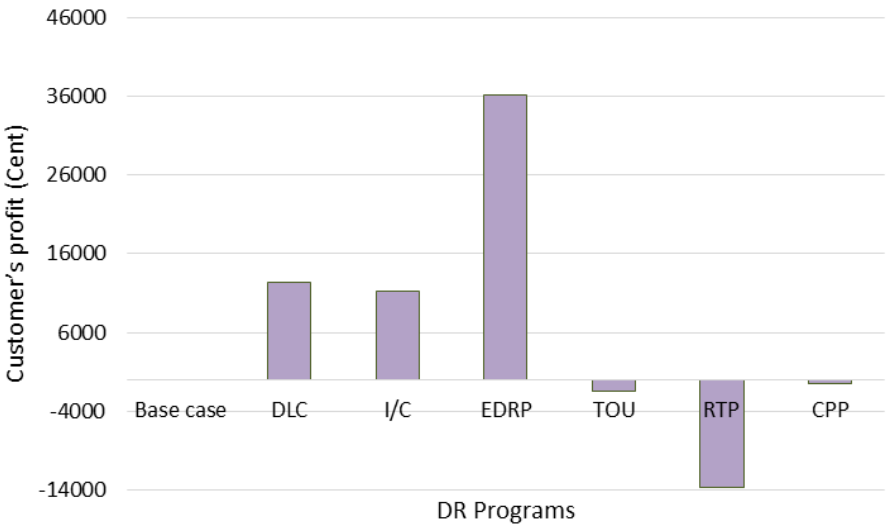

Fig. 25: Customer's profit for different DRPs in the 14-bus MG

Besides, the EDRP with the highest profit for customers and an acceptable operation cost seems to be the best choice; however, based on Fig. 26 and Table 8, it ranks lower in terms of peak reduction and other indices. In order to reach a better concept of operating cost reduction for EDRP compared to the base case (case 1), the power exchange of MG with the upstream for day eight is shown in Fig. 27. As it can be illustrated, a load reduction by customers during hours in which both of the load demand and energy price experience their peak values, provides an opportunity for the system operator to compensate a share of operating costs by employing local generation units and selling energy to the upstream grid (green curve). The priority list of DRPs based on the weighting

approach is shown in Fig. 28. Obviously, the EDRP is the best choice for critical operating times and also conditions with the high amount of uncertainties. The DLC and I/C seem to provide similar performances as the next options and afterward, the CPP and TOU as the next ranks. The RTP ranks the last due to a high expense for the customers.

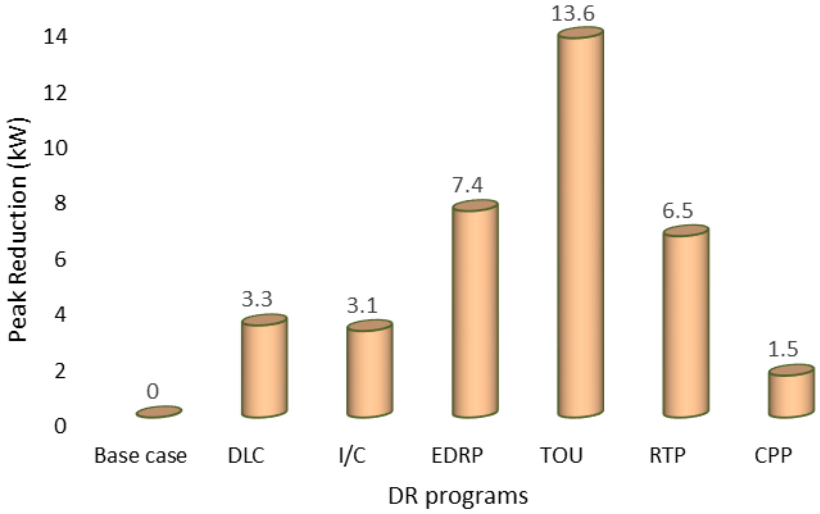

Fig. 26: Peak reduction for different DRPs in the 14-bus MG

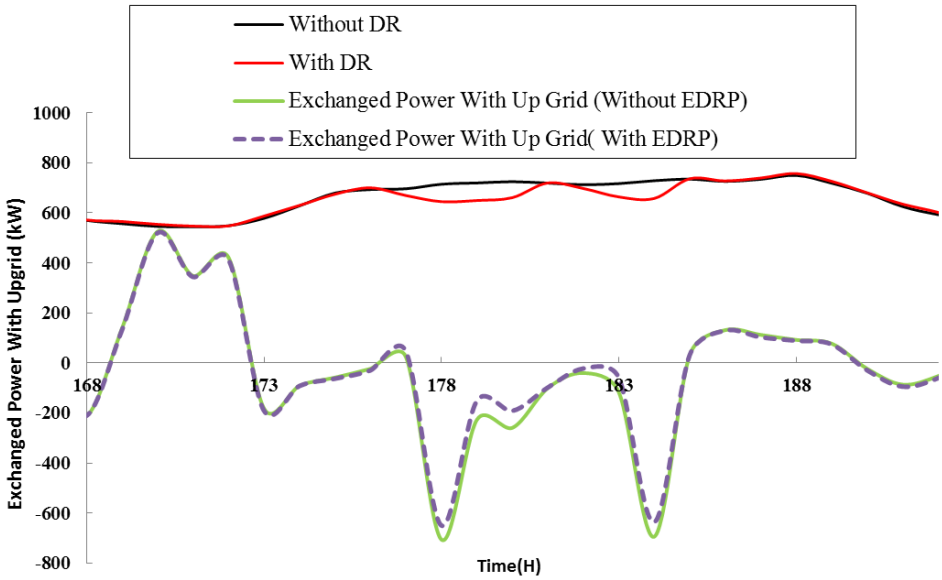

Fig. 27: Exchanged power with up-grid in the 14-bus MG

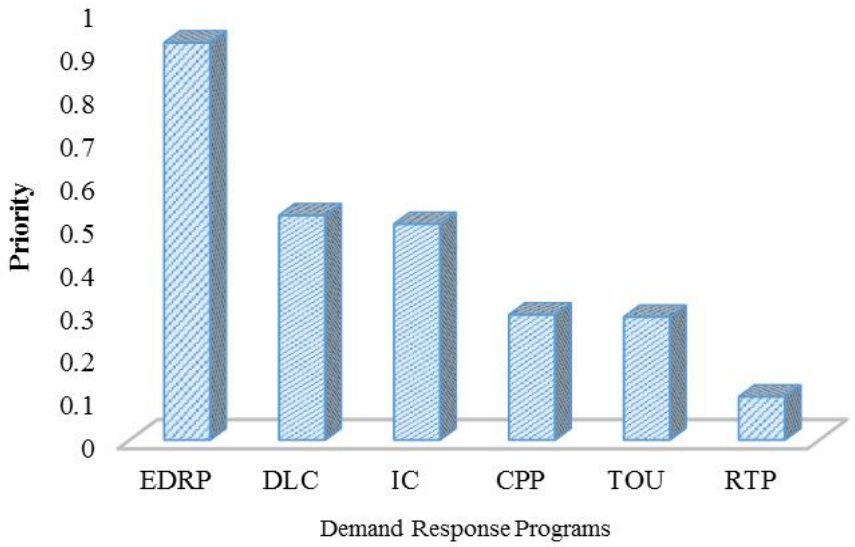

Fig. 28: Ranking of DRPs for the 14-bus MG

5 CONCLUSION

In this paper, the performance of two main categories of DRPs including incentive-based programs and time-based programs based on price elasticity and the customer benefit on the MG has been investigated. Moreover, penalties for customers in case of not to respond to the load reduction are considered. By using the proposed model, the operator can prioritize different DRPs for running in the MG. Simulations have been conducted on the 11-bus and 14-bus MGs. Uncertainties are modeled related to the DGs failure, inaccessibility to the upstream grid, load demand prediction, forecasted power of WT and PV units, and customer response to the curtailment program in order to approach the reality of MG operation. Based on the obtained results, the total operation cost is decreased in all cases after implementing DRPs. A priority list for the proposed DRPs has been provided. Although these priority lists are not exactly the same for both of the test systems, it can be deduced that EDRP, DLC and I/C are superior programs. After running DRPs for the 11-bus MG, it can be concluded that EDRP is the best option in critical times. The DLC and I/C have a similar efficiency as the next options, and then the RTP and TOU have the next ranks. For the 14-bus MG, it can be seen the RTP has the lowest operation cost while it provides the maximum cost for customers. As a result, the EDRP with the highest profit for customers and an acceptable operation cost seems to be the best choice. Needless to say, the advantage of EDRP is inevitable in MGs with high penetrations of renewable based DGs and power grids which are associated with considerable amounts of uncertainties; while other DRPs like DLC and I/C are appropriate choices if no better program is applicable. The results confirm that the peak reduction and the load demand shifting as two of the main objectives of DR implementation have been achieved for all the cases. In this study, because of considering most important uncertainties, the results are close to the real conditions, which provides MG operators and MG planners a general and practical overview for optimal

operation of the network.

REFERENCES

[1] N. W. A. Lidula and A. D. Rajapakse, "Microgrids research: A review of experimental microgrids and test systems," Renewable and Sustainable Energy Reviews, vol. 15, pp. 186-202, 2011

[2] T. Funabashi, T. Tanabe, T. Nagata, and R. Yokoyama, "An autonomous agent for reliable operation of power market and systems including microgrids," IEEE Electric Utility Deregulation and Restructuring and Power Technologies, pp. 173-177, 2008.

[3] D. Rui and G. Deconinck, "Market mechanism of smart grids: Multi-agent model and interoperability," IEEE Conference Networking, Sensing and Control (ICNSC), pp. 8-13, 2011

[4] A. L. Dimeas and N. D. Hatziargyriou, "Operation of a Multiagent System for Microgrid Control," Power Systems, IEEE Transactions on, vol. 20, pp. 1447-1455, 2005

[5] A. G. Tsikalakis and N. D. Hatziargyriou, "Centralized Control for Optimizing Microgrids Operation," Energy Conversion, IEEE Transactions on, vol. 23, pp. 241-248, 2008

[6] U. S. Department of Energy, "Energy policy Act of 2005", section 1252, February 2006

[7] Mazidi, Mohammadreza, et al. "Integrated scheduling of renewable generation and demand response programs in a microgrid." Energy Conversion and Management 86 (2014): 1118-1127.

[8] John H. Doudna, P.E," Overview of California ISO Summer 2000 Demand Response Programs ," IEEE, 2001

[9] S. Valero, M. Ortiz, C. Senabre, C. Alvarez, F. J. G, Franco, and A. Gabaldon, "Methods for customer and demand response policies selection in new electricity markets", IET Generation, Transmission & Distribution, vol. 1, no. 1, pp. 104-110, 2007

[10] E. Bompard, Y, Ma, R. Napoli, and G. Abrate, "The demand elasticity impacts on the strategic bidding behavior of the electricity producers", IEEE Transaction on Power Systems, vol. 22, no. 1, pp. 188-197, 2007.

[11] Aghaei, Jamshid, et al. "Contribution of emergency demand response programs in power system reliability." Energy 103 (2016): 688-696.

[12] Imani, M. Hosseini, Payam Niknejad, and M. R. Barzegaran. "The impact of customers' participation level and various incentive values on implementing emergency demand response program in microgrid operation." International Journal of Electrical Power & Energy Systems 96 (2018): 114-125.

[13] Dehnavi, Ehsan, and Hamdi Abdi. "Optimal pricing in time of use demand response by integrating with dynamic economic dispatch problem." Energy 109 (2016): 1086-1094.

[14] Aalami, H., G. R. Yousefi, and M. Parsa Moghadam. "Demand response model considering EDRP and TOU programs." Transmission and Distribution Conference and Exposition, 2008. T&D. IEEE/PES. IEEE, 2008.

[15] Shariatzadeh, Farshid, Paras Mandal, and Anurag K. Srivastava. "Demand response for sustainable energy systems: A review, application and implementation strategy." Renewable and Sustainable Energy Reviews 45 (2015): 343-350.

[16] Wang, Jianxiao, et al. "Distributed real-time demand response based on Lagrangian multiplier optimal selection approach." Applied Energy 190 (2017): 949-959.

[17] Aalami, H., G. R. Yousefi, and M. Parsa Moghadam. "A MADM-based support system for DR programs." Universities Power Engineering Conference, 2008. UPEC 2008. 43rd International. IEEE, 2008.

[18] Aalami, H. A., M. Parsa Moghaddam, and G. R. Yousefi. "Demand response modeling considering interruptible/curtailable loads and capacity market programs." Applied Energy 87.1 (2010): 243-250.

[19] Reihani, Ehsan, et al. "A novel approach using flexible scheduling and aggregation to optimize demand response in the developing interactive grid market architecture." Applied Energy 183 (2016): 445-455.

[20] Imani, Mahmood Hosseini, et al. "Running direct load control demand response program in microgrid by considering optimal position of storage unit." Texas Power and Energy Conference (TPEC), 2018 IEEE. IEEE, 2018.

[21] H. Aalami, et al., "Modeling and prioritizing demand response programs in power markets," Electric Power Systems Research, vol. 80, pp. 426-435, 2010.

[22] Nguyen, D. T., & Le, L. B. (2015). Risk-constrained profit maximization for microgrid aggregators with demand response. IEEE Transactions on Smart Grid, 6(1), 135-146.

[23] Geramifar, Hasan, Majid Shahabi, and Taghi Barforoshi. "Coordination of Energy Storage Systems and Demand Response Resources for Optimal Scheduling of Microgrids under Uncertainties." IET Renewable Power Generation (2016).

[24] Korkas, Christos D., Simone Baldi, Iakovos Michailidis, and Elias B. Kosmatopoulos. "Occupancy-based demand response and thermal comfort optimization in microgrids with renewable energy sources and energy storage." Applied Energy 163 (2016): 93-104.

[25] Chang, Chih-Lun, and Jimmy Chih-Hsien Peng. "A Decision-Making Auction Algorithm for Demand Response in Microgrids." IEEE Transactions on Smart Grid (2016).

[26] Aghajani, G. R., H. A. Shayanfar, and H. Shayeghi. "Demand side management in a smart micro-grid in the presence of renewable generation and demand response." Energy 126 (2017): 622-637.

[27] Zhang, Cuo, et al. "Robust Coordination of Distributed Generation and Price-Based Demand Response in Microgrids." IEEE Transactions on Smart Grid (2017).

[28] Pourmousavi, S. Ali, M. Hashem Nehrir, and Ratnesh K. Sharma. "Multi-timescale power management for islanded microgrids including storage and demand response." IEEE Transactions on Smart Grid 6.3 (2015): 1185-1195.

[29] M. H. Albadi and E. El-Saadany, "Demand response in electricity markets: An overview," in IEEE power engineering society general meeting, 2007, pp. 1-5.

[30] Kirschen DS, Strbac G. Fundamentals of power system economics. John Wiley & Sons; 2004.

[31] R. Karki, et al., "A simplified wind power generation model for reliability evaluation," Energy conversion, IEEE Transactions on, vol. 21, pp. 533-540, 2006.

[32] Wang, Jianhui, Mohammad Shahidehpour, and Zuyi Li. "Security-constrained unit commitment with volatile wind power generation." IEEE Transactions on Power Systems23.3 (2008): 1319-1327.

[33] Khodayar, Mohammad E., Lei Wu, and Mohammad Shahidehpour. "Hourly coordination of electric vehicle operation and volatile wind power generation in SCUC." IEEE Transactions on Smart Grid 3.3 (2012): 1271-1279.

[34] Chen, Changsong, et al. "Smart energy management system for optimal microgrid economic operation." IET renewable power generation 5.3 (2011): 258-267.

[35] A. A. Moghaddam, et al., "Multi-operation management of a typical micro-grids using Particle Swarm Optimization: A comparative study," Renewable and Sustainable Energy Reviews, vol. 16, pp. 1268-1281, 2012.

[36] L. Lu and P. Liu, "Research and simulation on photovoltaic power system maximum power control," in Electrical and Control Engineering (ICECE), 2011 International Conference on, 2011, pp. 1394-1398.

[37] Shahidehpour, M. (2012). "Operation and Control Microgrid and Distributed Generation." Illinois Instit ute of Technology.

[38] X. Xu, et al., "Evaluation of Operational Reliability of a Microgrid Using a Short-Term Outage Model," Power Systems, IEEE Transactions on, vol. 29, pp. 2238-2247, 2014.

[39] A. Zakariazadeh, et al., "Smart microgrid energy and reserve scheduling with demand response using stochastic optimization," International Journal of Electrical Power & Energy Systems, vol. 63, pp. 523-533, 2014.

[40] [Online]. Available: http://www.gams.com/

[41] [Online] Available at: http://www.bluesunpv.com

[42] L. Wu, et al., "Stochastic security-constrained unit commitment," Power Systems, IEEE Transactions on, vol. 22, pp. 800-811, 2007.

[43] [Online]. Available: http://www.nrel.gov/

[44] [Online]. Available: http://www.ieso.ca/Pages/Power-Data